

NEBULAR: A Simple Synthesis Code for the Hydrogen and Helium Nebular Spectrum

M. Schirmer

Gemini Observatory, Casilla 603, La Serena, Chile

`mschirme@gemini.edu`

ABSTRACT

NEBULAR synthesizes an accurate spectrum of an ideal, mixed hydrogen and helium gas in ionization equilibrium, over a useful range of densities, temperatures and wavelengths. Free-free, free-bound and two-photon continua are included as well as parts of the H I, He I and He II line series. NEBULAR interpolates over publicly available data tables. Amongst other purposes, the resulting spectra can be used to determine equivalent line widths, constrain the contribution of the nebular continuum to some bandpass, and for educational purposes.

Subject headings: ISM: general, methods: numerical

1. Introduction

Powerful computer codes such as CLOUDY (Ferland et al. 2013) synthesize realistic spectra of arbitrary astrophysical nebulae. These codes may have complex setups and significant execution times because of their ambitious scope.

NEBULAR is not a contender in this area. It quickly synthesizes an accurate and fairly complete spectrum of an ideal, mixed hydrogen and helium gas in ionization equilibrium, over a wide range of temperatures, densities and wavelengths. It also provides easy access to the most recent atomic computations.

NEBULAR is open source and licenced under the GNU Public Licence (GPL). It is written in C++ and links against common standard libraries, facilitating cross-platform usability and installation.

2. Methods and limitations of the code

The combined hydrogen and helium spectrum is synthesized from four different components: the free-bound, free-free and two-photon continua, and part of the H I, He I and He II emission line series. The respective rescaled emission coefficients

j are written as

$$j_{\text{fb}}(\nu) = \frac{1}{4\pi} N_X N_e \gamma_{\text{fb}}(\nu) \quad (1)$$

$$j_{\text{ff}}(\nu) = \frac{1}{4\pi} N_X N_e \gamma_{\text{ff}}(\nu) \quad (2)$$

$$j_{2\text{q}}(\nu) = \frac{1}{4\pi} N_X N_e \gamma_{2\text{q}}(\nu) \quad (3)$$

$$j_{\text{nn}'} = \frac{1}{4\pi} N_X N_e \gamma_{\text{nn}'} \quad (4)$$

Here, N_X and N_e are the ion and electron number densities in cm^{-3} , respectively, and γ is the emission coefficient (in $\text{erg s}^{-1} \text{cm}^3 \text{Hz}^{-1}$; apart from $j_{\text{nn}'}$, which has no frequency dependence).

The sources of the input data, as well as the limitations of the code, are reviewed below.

2.1. Free-bound continuum

Free-bound emission is caused by ions capturing free electrons. Ercolano & Storey (2006) have tabulated the continuous free-bound recombination emission coefficients, γ_{bf} , of H I, He I and He II (the ionic states after recombination) over $10^2 \leq T \leq 10^5$ K with a step size of $\Delta \log(T) = 0.1$. NEBULAR performs a cubic spline interpolation over temperatures, and a linear interpolation over frequencies within discontinuities. As stated

Table 1: Validity matrix for NEBULAR. Extrapolation may be used outside these ranges.

Component	Temperatures	Densities	Wavelength range
	T [K]	$\log(N_e/\text{cm}^{-3})$	
Free-bound (H I)	10^{2-5}	–	911.8 Å–36.5 μm
Free-bound (He I)	10^{2-5}	–	504.3 Å–36.5 μm
Free-bound (He II)	10^{2-5}	–	228.0 Å–36.5 μm
Free-free (all)	$3 - 10^{10}$	–	Radio to γ-rays
Two-photon (H I)	$10^{2.5-5}$	$\lesssim 8$	1215.7 Å–∞
Two-photon (He I)	5000 – 20000	–	625 Å–∞
Two-photon (He II)	$10^{3.0-5}$	$\lesssim 8$	303.9 Å–∞
H I lines	500 – 30000	2 – 8	911.7 Å–27.8 μm
He I lines	5000 – 25000	1 – 14	2945 Å–2.16 μm
He II lines	500 – 100000	2 – 8	227.9 Å–34.6 μm

in Ercolano & Storey (2006), bilinear interpolation reproduces the true values to within 1% or better.

2.2. Free-free continuum

Free-free emission is caused by electrons scattering in the Coulomb field of ions with nuclear charge Z . NEBULAR computes the free-free spectrum for H^+ , He^+ and He^{++} . The emission coefficients are

$$j_{ff}(\nu) = \frac{1}{4\pi} N_X N_e \frac{32 Z^2 e^4 h}{3 m_e^2 c^3} \left(\frac{\pi h \nu_0}{3 k_B T} \right)^{1/2} \times \exp(-h\nu/k_B T) g_{ff}(Z, T, \nu) \quad (5)$$

(e.g. Brown & Mathews 1970). Here, e , m_e , h , and k_B are the electron charge, electron mass, Planck constant and Boltzmann constant, respectively. $h\nu_0$ denotes the ionization energy for hydrogen. Note that this equation must be evaluated in cgs units, in particular the electronic charge is $1e = 4.803207 \times 10^{-7}$ statC, with $1\text{statC} = 1\text{cm}^{3/2}\text{g}^{1/2}\text{s}^{-1}$.

$g_{ff}(Z, T, \nu)$ is the Gaunt factor, a quantum mechanical correction to the classical scattering formalism. For typical conditions in astrophysical nebulae, $g_{ff} \sim 1 - 2$. Non-relativistic Gaunt factors have been calculated by van Hoof et al. (2014) for a wide range of temperatures, frequencies and nuclear charges. NEBULAR uses the tabulated temperature-averaged $\langle g_{ff}(\gamma^2, u) \rangle$ for Maxwell-Boltzmann electron distributions, where $\gamma^2 = Z^2 h\nu_0/(k_B T)$ and $u = h\nu/(k_B T)$.

The data for $\langle g_{ff}(\gamma^2, u) \rangle$ are available on a log-log grid with regular step sizes in both dimensions.

NEBULAR interpolates this grid using a 2D bicubic interpolation from the GNU Scientific Library (GSL v2.1).

2.3. Two-photon continuum

2.3.1. H I and He II

The 2^2S level in hydrogenic ions can e.g. be populated by direct recombinations onto that level, and by downward cascades following electron capture to a higher level. A radiative decay to the 1^2S level is forbidden by the dipole selection rules (Laporte & Meggers 1925). However, the transition may occur if *two* photons are emitted whose energies add up to the Lyman- α ($\text{Ly}\alpha$) energy. The transition probability for the hydrogenic $2S \rightarrow 1S$ two-photon decay is

$$A_{2q} = 8.2249 Z^6 \frac{R_Z}{R_H} \text{s}^{-1} \quad (6)$$

(Nussbaumer & Schmutz 1984). Two-photon decays from higher levels (Hirata 2008) are ignored, as they contribute on the sub-percent level, only.

The two-photon spectrum has a natural upper cut-off at the $\text{Ly}\alpha$ frequency. It peaks at half the $\text{Ly}\alpha$ frequency when expressed in frequency units, emphasizing the importance of this process for near- and far-UV observations. For low densities, the hydrogen two-photon emission exceeds the free-bound continuum (Sect. 2.1) at wavelengths of around $\text{H}\beta$ (4863 Å) and below (Fig. 1).

The two-photon emission coefficient is

$$\gamma_{2q}(\nu) = \alpha_{2^2S}^{\text{eff}}(T, N_e) g(\nu) \left(1 + \frac{\sum_X N_X q^X}{A_{2q}} \right)^{-1} \quad (7)$$

(e.g. Osterbrock & Ferland 2006). The individual factors are discussed in the following.

Effective recombination coefficient to 2^2S

$\alpha_{2^2S}^{\text{eff}}(T, N_e)$ is the effective recombination coefficient to the 2^2S level. It has been tabulated for both H I and He II by Hummer & Storey (1987) over wide temperature and density ranges (Case B, only). The coefficients from the original publication were extracted and digitized, and are reproduced in the Appendix (Tables 2 and 3). For convenience, these tables contain the coefficients for the 2^2P level as well, so that the total $n = 2$ effective recombination coefficient may be calculated (not needed for the two-photon emission). For H I, NEBULAR extrapolates $\alpha_{2^2S}^{\text{eff}}(T, N_e)$ from $\log(T) = 3.0$ to 2.5, from $\log(T) = 4.5$ to 5.0, and from $\log(N_e) = 2.0$ to 0.0. For He II, extrapolation is used from $\log(T) = 3.5$ to 3.0, and from $\log(N_e) = 2.0$ to 0.0. These extrapolations are expected to be accurate within a few percent, as the functional dependence of $\alpha_{2^2S}^{\text{eff}}(T, N_e)$ at these densities and temperatures is weak.

Frequency dependence

The frequency dependence of the two-photon spectrum is absorbed in

$$g(\nu) = h \frac{\nu}{\nu_\alpha} A\left(\frac{\nu}{\nu_\alpha}\right) / A_{2q}. \quad (8)$$

Here, ν_α is the Ly α frequency of the respective hydrogenic ion. Nussbaumer & Schmutz (1984) have presented an analytical fit for the frequency dependent transition probability, $A(\nu/\nu_\alpha)$. It is accurate to within 1% over nearly the full spectral range,

$$A(\nu/\nu_\alpha) = C [y(1 - (4y)^\gamma) + \alpha y^\beta (4y)^\gamma], \quad (9)$$

with $y = \frac{\nu}{\nu_\alpha} (1 - \frac{\nu}{\nu_\alpha})$, $\alpha = 0.88$, $\beta = 1.53$, $\gamma = 0.8$ and $C = 202.0 Z^6 R_Z/R_H \text{ s}^{-1}$, where Z is the nuclear charge.

Collisional de-population of the 2^2S level

The 2^2S level can be de-populated by means of angular momentum changing (l -changing) collisions, $2^2S \rightarrow 2^2P$, inflicted by other ions and electrons. The 2^2P level may then decay radiatively to the 1^2S level by emitting a Ly α photon, reducing the two-photon flux. This is described by the collisional transition rate coefficients, $q^X(T, N_e)$. Rates for l -changing collisions at a fixed principal quantum number $n = 2$ are much higher than for n -changing collisions, and $n = 2 \rightarrow 3$ collisions typically require $N_e \gtrsim 10^6 \text{ cm}^{-3}$ (e.g. Hummer & Storey 1987). Therefore, n -changing collisions are ignored.

Pengelly & Seaton (1964) have developed a theory to calculate these collisional transition rates. Vranceanu et al. (2012) have argued that these rates are significantly overestimated. This, however, has been disputed by Storey & Sochi (2015) and Guzmán et al. (2016). Consequently, NEBULAR uses the prescription of Pengelly & Seaton (1964). Accordingly, the hydrogen two-photon emissivity becomes significantly reduced for $N_X \gtrsim 1000 \text{ cm}^{-3}$.

2.3.2. The He I two-photon continuum

The $1s2s\ 1S$ and $1s2s\ 3S$ states in He I may also decay by two-photon emission to the ground state (Drake et al. 1969). The decay rates for $1s2s\ 3S$ are ignored, as they are about 10 orders of magnitude lower than for the $1S$ state. The total transition probability is

$$A_{2q} = 53.1 \text{ s}^{-1} \quad (10)$$

for $1s2s\ 1S$. In analogy to Nussbaumer & Schmutz (1984), the spectral dependence tabulated in Drake et al. (1969) is approximated in NEBULAR,

$$A(y) = C[1 + \beta(y - 1/2)^2 + \gamma(y - 1/2)^4], \quad (11)$$

with $y = \nu/\nu_0$, $\alpha = 145.29 \text{ s}^{-1}$, $\beta = -2.259$ and $\gamma = -8.77$. This fit is accurate to 0.9% or better over $0.025 \leq y \leq 0.975$.

The rest of the treatment is the same as outlined in Sect. 2.3.1, with the notable distinction that no extensive data are available for $\alpha^{\text{eff}}(T, N_e)$. While CLOUDY calculates these parameters internally, NEBULAR relies on the single temperature dependence between 5000 – 20000 K listed in Golovatyj et al. (1997). Fortunately, this is not a big

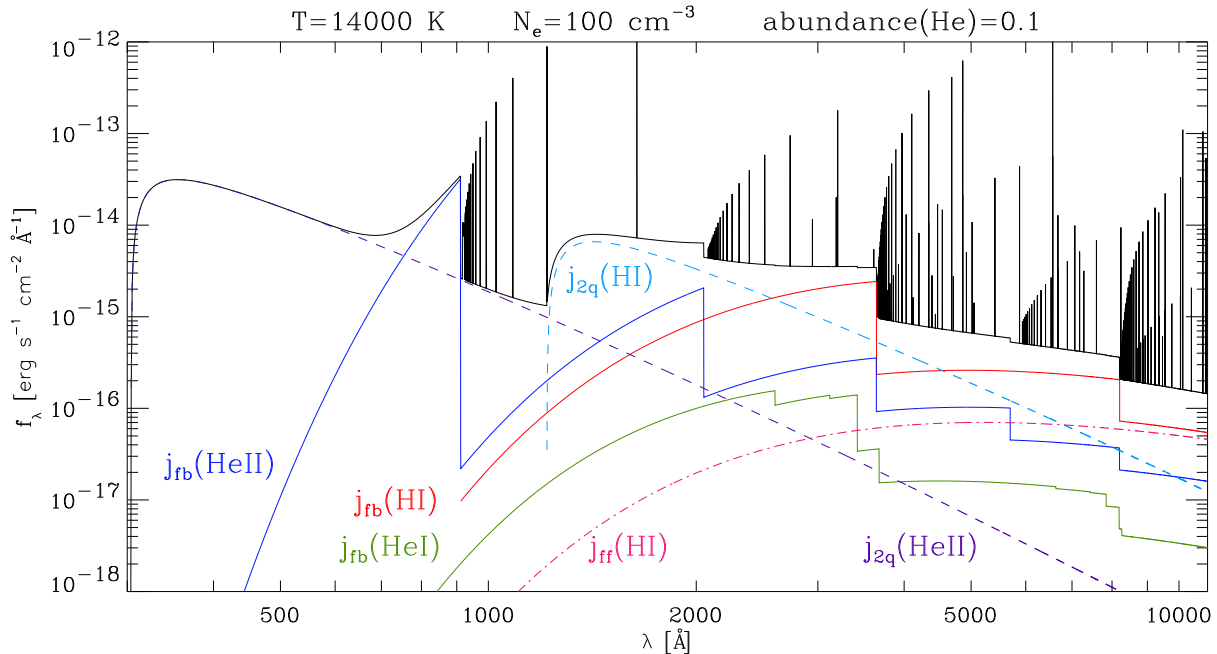


Fig. 1.— Example total output spectrum (top thick solid line, including the emission line series). The other three solid lines with the characteristic ionisation edges represent the free-bound contributions by H I, He I and He II. The two dashed lines display the two-photon continua (H I and He II), and the lower dash-dotted line the H I free-free emission.

drawback: for typical abundances and depending on T , the He I two-photon continuum is 2–6 orders of magnitude below the H I two-photon continuum. Peak emission in f_λ occurs at around 770 nm.

2.4. Emission lines

2.4.1. H I emission lines

The H I emission line spectrum for Case B (Lyman-thick nebulae) is built from Storey & Sochi (2015) and includes all line transitions from upper levels $n \leq 99$ onto lower levels $n' \leq 8$. The latter was chosen so that the α line of a $j_{nn'}$ series has a wavelength shorter than $36 \mu\text{m}$, i.e. it still falls within the free-bound continuum calculated by Ercolano & Storey (2006). The parameter space covers $\log(N_e) = 2-6$ and $\log(T) = 2.0-4.4$. The Lyman series ($n' = 1$) is excluded for Case B.

Linear extrapolation is used to cover the $\log(N_e) = 0-2$ range. The extrapolation has been verified by comparison with Pengelly (1964) for $\log(N_e) = 0$ and $T = 1250-80000$ K. The

extrapolation is accurate to 2.5% or better for $T = 2500-40000$ K. For $T = 1250$ K and $T = 80000$ K, the errors are 4% and 7%, respectively. Calculations of the H I line spectrum are limited to upper levels of $n \leq 25$ (Storey & Hummer 1995) if extrapolation is used, and are skipped for $T > 50000$ K.

For Case A (Lyman-thin nebulae), the emission coefficients are taken from Storey & Hummer (1995). The same limitations hold as outlined above; the Lyman series ($n' = 1$) is included.

2.4.2. He II emission lines

The He II spectrum for Case A+B is based on Storey & Hummer (1995), with a common upper level of $n \leq 25$. Treatment is the same as outlined for H I, with some differences: First, transitions onto lower levels $n' \leq 14$ are included. Second, the temperature range is limited to $500 \leq T \leq 10^5$ K. Third, calculations are skipped if $T > 10^5$ K.

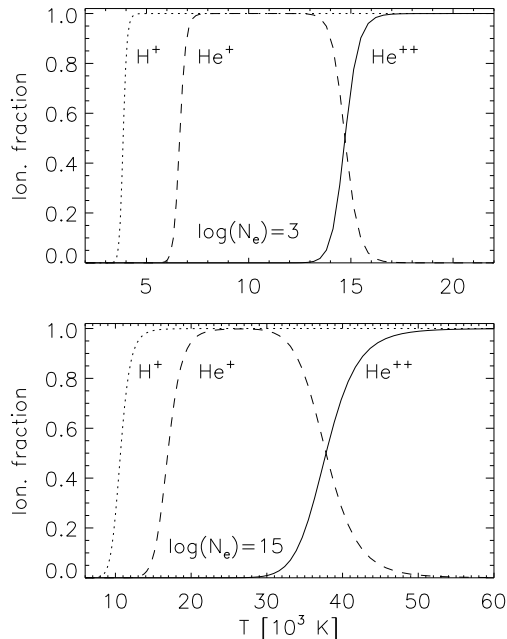


Fig. 2.— Hydrogen and helium ionization fractions for $N_e = 10^3 \text{ cm}^{-3}$ and 10^{15} cm^{-3} , as calculated by NEBULAR.

2.4.3. He I emission lines

The data from Porter et al. (2013) are used (corrigendum to Porter et al. 2012) to construct the He I spectrum for $T = 5000 - 25000 \text{ K}$, $\log(N_e) = 1 - 14$, and Case B. In total, 44 singlet and triplet lines are available between $2945 - 21617 \text{ \AA}$.

2.4.4. Other remarks

Storey & Hummer (1995) and Storey & Sochi (2015) have provided data servers to access and interpolate their data tables. These servers are not directly useful for NEBULAR because of their interactive nature. They were used to extract the data on the pre-defined $(\log(N_e), \log(T))$ grid points. As the original grids are not strictly regular, Mathematica was used to build a regular grid, enabling bicubic 2D GSL interpolation for NEBULAR. Within rounding errors, NEBULAR yields the same results as the original data servers.

Recently, it has been discussed that the energy distributions of free electrons may not follow a purely thermal Maxwell-Boltzmann distribution (e.g. Storey & Sochi 2015; Zhang et al.

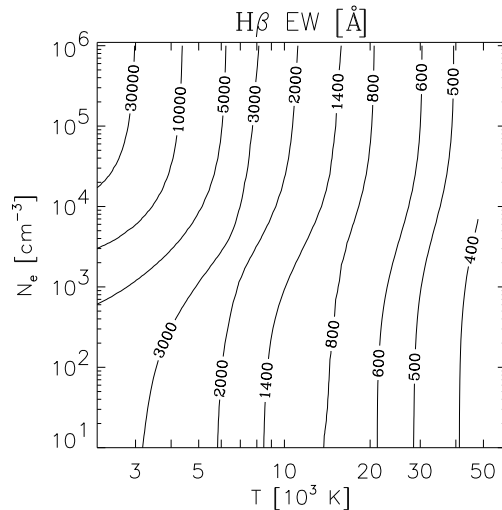


Fig. 3.— $H\beta$ equivalent width over the full nebular continuum, as a function of N_e and T , for a helium abundance of 0.1 by parts.

2015). At this point, NEBULAR adopts Maxwell-Boltzmann distributions throughout.

2.5. Ionization fractions

The ionization fractions of H^+ , He^+ and He^{++} (and their number densities, N_X), are calculated for a mixed H/He plasma in ionization equilibrium, solving the Saha equation similar to Rouse (1962). Therein, the algorithm starts with a fixed matter density ρ , and then iteratively obtains N_e ; the ionization fractions follow. In the case of NEBULAR, the iteration is skipped as N_e is a fixed parameter. Figure 2 shows these ionization fractions, calculated for a low and a high density mix. Alternatively, user-defined estimates for the ionization fractions can be given to NEBULAR as command-line arguments.

3. Usage and conclusions

3.1. Command-line arguments

NEBULAR is invoked on the command-line and controlled by mandatory and optional arguments (Table 4). If no arguments are given, NEBULAR reports its usage.

There are three mandatory arguments: a wavelength/frequency range including step size, the

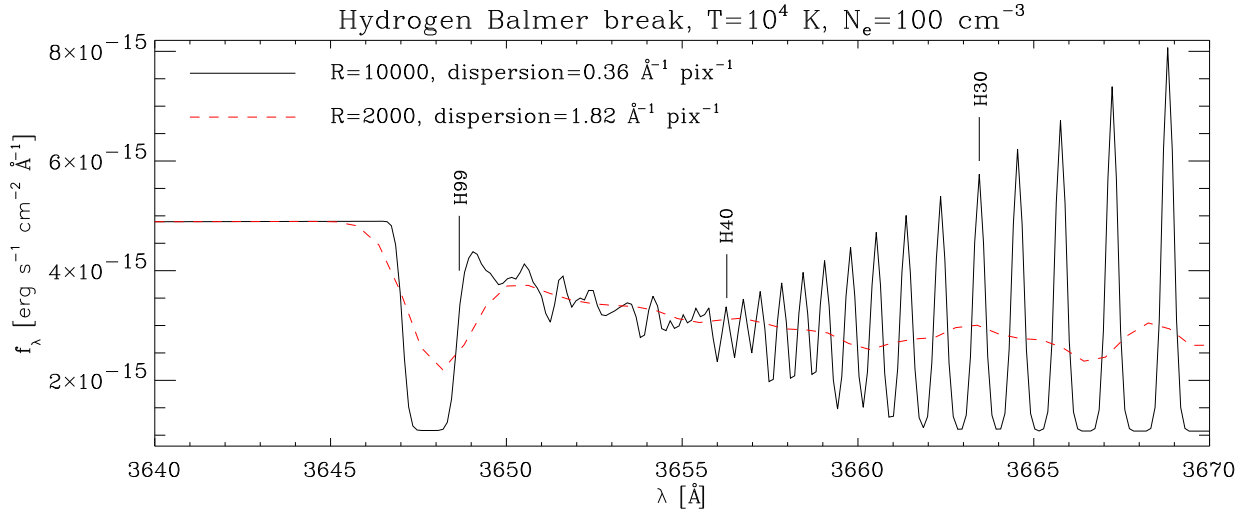


Fig. 4.— The hydrogen Balmer break at 3646\AA , as seen by two spectrographs with resolutions $R = 2000$ and $R = 10000$, respectively, calculated by `NEBULAR`. The confluent high-order Balmer lines form a pseudo-continuum, masking the discontinuous Balmer break. The broad minimum near the break is artificial, because upper levels $n \leq 99$, only, are available to `NEBULAR`.

electron density N_e , and the electron temperature T . The range is assumed to be a wavelength range in \AA if the numeric minimum and maximum values are less than 10^7 ; otherwise, frequencies [Hz] are assumed. Alternatively, a file containing an ASCII table may be provided, containing the wavelengths for e.g. each pixel of an observed spectrum.

3.2. Output

`NEBULAR` produces an ASCII table with the various components and the total spectrum evaluated at each wavelength (or frequency). The results can be readily displayed in `TOPCAT` (Taylor 2005).

If a wavelength range is given, then the output spectral flux density will be in wavelength units (f_λ , $\text{erg s}^{-1} \text{cm}^{-2} \text{\AA}^{-1}$). If frequencies are given, then the spectrum will be returned in frequency units (f_ν , $\text{erg s}^{-1} \text{cm}^{-2} \text{Hz}^{-1}$). Internally, all calculations are performed in frequency units. An excerpt of the output is shown in Table 5.

`NEBULAR` also prints various parameters to the header comment section of the output file, such as the derived ionization fractions, the ionic number densities, and the total physical gas density.

Pure hydrogen (helium) spectra can be produced by setting the abundance to 0 (1).

3.3. Summary

`NEBULAR` accurately synthesizes the nebular spectrum of an ideal H/He gas mix in ionization equilibrium over a wide range of densities, temperatures and wavelengths. For this purpose it uses recent and extensive atomic computations by others. To infer accurate physical parameters of a real, astrophysical nebula, full photoionization codes such as `CLOUDY` should be used.

The synthesis of a complete spectrum from $300 - 30000\text{\AA}$ with 0.1\AA resolution takes a few seconds on a 2 GHz CPU. This makes `NEBULAR` useful to study various quantitative and qualitative aspects of the spectrum, such as the relative contributions of the various continuum processes. One can also calculate the equivalent width of a particular emission line over the nebular continuum (e.g. Fig. 3), and then estimate the contribution of the continuum to some composite spectrum based on the observed line strength.

Usually, the nebular continuum is weak and often undetected in extragalactic observations. Yet it can become significant at UV wavelengths because of strong two-photon emission. If the continuum has been fixed based on optical observations of e.g. the $\text{H}\beta$ line, then its contribution

to the GALEX NUV and FUV bandpasses may be estimated. Another application would be the observational properties of the Balmer break at 3646Å, as a function of spectrograph resolution and dispersion. Figure 4 illustrates the blurring effect of the confluent high-order Balmer lines, effectively masking the Balmer jump (e.g. Lintott et al. 2009).

Acknowledgements

TBW.

REFERENCES

- Brocklehurst, M. 1971, MNRAS, 153, 471
- Brown, R. L. & Mathews, W. G. 1970, ApJ, 160, 939
- Drake, G. W., Victor, G. A., & Dalgarno, A. 1969, Physical Review, 180, 25
- Ercolano, B. & Storey, P. J. 2006, MNRAS, 372, 1875
- Ferland, G. J., Porter, R. L., van Hoof, P. A. M., et al. 2013, Rev. Mexicana Astron. Astrofis., 49, 137
- Golovatyj, V. V., Sapor, A., Feklistova, T., & Kholtygin, A. F. 1997, Astronomical and Astrophysical Transactions, 12, 85
- Guzmán, F., Badnell, N. R., Williams, R. J. R., et al. 2016, MNRAS
- Hirata, C. M. 2008, Phys. Rev. D, 78, 023001
- Hummer, D. G. & Storey, P. J. 1987, MNRAS, 224, 801
- Laporte, O. & Meggers, W. F. 1925, Journal of the Optical Society of America, 11, 459
- Lintott, C. J., Schawinski, K., Keel, W., et al. 2009, MNRAS, 399, 129
- Nussbaumer, H. & Schmutz, W. 1984, A&A, 138, 495
- Osterbrock, D. E. & Ferland, G. J. 2006, Astrophysics of gaseous nebulae and active galactic nuclei (University Science Books)
- Pengelly, R. M. 1964, MNRAS, 127, 145
- Pengelly, R. M. & Seaton, M. J. 1964, MNRAS, 127, 165
- Porter, R. L., Ferland, G. J., Storey, P. J., & Dettisch, M. J. 2012, MNRAS, 425, L28
- Porter, R. L., Ferland, G. J., Storey, P. J., & Dettisch, M. J. 2013, MNRAS, 433, L89
- Rouse, C. A. 1962, ApJ, 135, 599
- Spitzer, L. 1956, Physics of Fully Ionized Gases (Interscience Publishers)
- Storey, P. J. & Hummer, D. G. 1995, MNRAS, 272, 41
- Storey, P. J. & Sochi, T. 2015, MNRAS, 446, 1864
- Taylor, M. B. 2005, in Astronomical Society of the Pacific Conference Series, Vol. 347, Astronomical Data Analysis Software and Systems XIV, ed. P. Shopbell, M. Britton, & R. Ebert, 29
- van Hoof, P. A. M., Williams, R. J. R., Volk, K., et al. 2014, MNRAS, 444, 420
- Vrinceanu, D., Onofrio, R., & Sadeghpour, H. R. 2012, ApJ, 747, 56
- Zhang, Y., Zhang, B., & Liu, X.-W. 2015, ArXiv e-prints

Some mistakes, mostly of typographical nature, were found in the literature:

- In Table VI of Pengelly (1964) for the He II Pickering series, for $n = 19$, $t' = 1$ and Case B, it should read 0.39 instead of 3.39.
- Pengelly & Seaton (1964) erroneously have a factor of π^2 in the denominator for the Debye radius (their eq. 33). Correct would be a single factor π . Subsequent derivations and numeric evaluations, however, are correctly calculated.
- In their eq. (3.40), Brocklehurst (1971) also have a factor of π^2 in the denominator for the Debye radius, and carry it over in their calculations of the collision rates. Spitzer (1956) is cited for the equation, yet in that original work the dependence on π is linear. CLOUDY (v13.03) has the same wrong dependence on π^2 in the calculation of the collision rates, a bug that has been fixed in v15.
- In Table 4.2 of Osterbrock & Ferland (2006) the H I Paschen-line series, the values tabulated for $j_{P\delta}/j_{H\beta}$ actually refer to $j_{P\epsilon}/j_{H\beta}$. This table has been derived from Pengelly (1964), where this error is absent.
- In Table 4.3 of Osterbrock & Ferland (2006) the relative intensities with respect to He II $\lambda 4686$ are mistakenly a factor of 10 too low for $n \rightarrow 2$ and $T = 5000, 10000$ and 20000 K. This table has been reproduced from Storey & Hummer (1995), where this error is absent.

Table 2: Effective recombination coefficients to H I 2^2S (upper half) and H I 2^2P (lower half), see also Sect. 2.3. Extracted and reproduced from Table 8 in Hummer & Storey (1987). The total recombination coefficient for the $n = 2$ level is obtained by adding the 2^2S and 2^2P values.

	$\log(N_e / \text{cm}^{-3})$								
	2	3	4	5	6	7	8	9	10
T [K]	$\alpha_{\text{HI}2^2S}^{\text{eff}} [\text{cm}^3 \text{s}^{-1}]$								
1000	3.594e-13	3.701e-13	3.891e-13	4.226e-13	4.814e-13	5.887e-13	7.959e-13	1.163e-12	1.842e-12
3000	1.843e-13	1.861e-13	1.894e-13	1.950e-13	2.047e-13	2.211e-13	2.491e-13	2.846e-13	3.091e-13
5000	1.334e-13	1.341e-13	1.354e-13	1.377e-13	1.416e-13	1.481e-13	1.592e-13	1.710e-13	1.679e-13
7500	1.020e-13	1.023e-13	1.029e-13	1.039e-13	1.057e-13	1.087e-13	1.137e-13	1.182e-13	1.101e-13
10000	8.373e-14	8.390e-14	8.422e-14	8.477e-14	8.571e-14	8.729e-14	9.006e-14	9.210e-14	8.350e-14
12500	7.152e-14	7.162e-14	7.180e-14	7.213e-14	7.267e-14	7.358e-14	7.525e-14	7.621e-14	6.807e-14
15000	6.268e-14	6.274e-14	6.285e-14	6.305e-14	6.337e-14	6.392e-14	6.497e-14	6.540e-14	5.790e-14
20000	5.059e-14	5.061e-14	5.065e-14	5.072e-14	5.083e-14	5.102e-14	5.147e-14	5.144e-14	4.513e-14
30000	3.690e-14	3.690e-14	3.690e-14	3.689e-14	3.686e-14	3.682e-14	3.687e-14	3.665e-14	3.204e-14
T [K]	$\alpha_{\text{HI}2^2P}^{\text{eff}} [\text{cm}^3 \text{s}^{-1}]$								
1000	1.151e-12	1.163e-12	1.187e-12	1.235e-12	1.328e-12	1.512e-12	1.912e-12	2.947e-12	5.979e-12
3000	4.854e-13	4.865e-13	4.890e-13	4.943e-13	5.049e-13	5.265e-13	5.703e-13	6.760e-13	9.467e-13
5000	3.185e-13	3.189e-13	3.197e-13	3.216e-13	3.254e-13	3.331e-13	3.489e-13	3.880e-13	4.919e-13
7500	2.251e-13	2.253e-13	2.257e-13	2.265e-13	2.281e-13	2.316e-13	2.386e-13	2.566e-13	3.080e-13
10000	1.747e-13	1.748e-13	1.750e-13	1.755e-13	1.764e-13	1.784e-13	1.823e-13	1.926e-13	2.247e-13
12500	1.429e-13	1.429e-13	1.430e-13	1.434e-13	1.440e-13	1.453e-13	1.478e-13	1.545e-13	1.771e-13
15000	1.208e-13	1.209e-13	1.210e-13	1.212e-13	1.217e-13	1.226e-13	1.243e-13	1.290e-13	1.461e-13
20000	9.220e-14	9.222e-14	9.229e-14	9.243e-14	9.272e-14	9.329e-14	9.425e-14	9.687e-14	1.080e-13
30000	6.217e-14	6.219e-14	6.223e-14	6.231e-14	6.247e-14	6.276e-14	6.319e-14	6.427e-14	7.047e-14

Table 3: Effective recombination coefficients to He II 2^2S (upper half) and He II 2^2P (lower half). Extracted and reproduced from Table 9 in Hummer & Storey (1987).

T [K]	$\log(N_e / \text{cm}^{-3})$											
	2	3	4	5	6	7	8	9	10	11	12	13
	$\alpha_{\text{HeII } 2^2S}^{\text{eff}} [\text{cm}^3 \text{s}^{-1}]$											
3000	8.296e-13	8.373e-13	8.552e-13	8.887e-13	9.487e-13	1.056e-12	1.250e-12	1.627e-12	2.425e-12	4.072e-12	8.155e-12	2.670e-11
5000	6.174e-13	6.207e-13	6.287e-13	6.439e-13	6.712e-13	7.189e-13	8.029e-13	9.551e-13	1.246e-12	1.737e-12	2.632e-12	5.930e-12
7500	4.859e-13	4.876e-13	4.917e-13	4.997e-13	5.140e-13	5.390e-13	5.821e-13	6.578e-13	7.949e-13	9.944e-13	1.272e-12	2.244e-12
10000	4.091e-13	4.101e-13	4.126e-13	4.176e-13	4.265e-13	4.421e-13	4.688e-13	5.149e-13	5.962e-13	7.030e-13	8.167e-13	1.246e-12
12500	3.572e-13	3.578e-13	3.596e-13	3.630e-13	3.691e-13	3.798e-13	3.980e-13	4.292e-13	4.863e-13	5.492e-13	5.996e-13	8.298e-13
15000	3.190e-13	3.195e-13	3.208e-13	3.232e-13	3.277e-13	3.355e-13	3.487e-13	3.713e-13	4.103e-13	4.542e-13	4.748e-13	6.122e-13
20000	2.659e-13	2.661e-13	2.669e-13	2.683e-13	2.710e-13	2.756e-13	2.835e-13	2.968e-13	3.197e-13	3.423e-13	3.381e-13	3.961e-13
30000	2.036e-13	2.037e-13	2.041e-13	2.047e-13	2.059e-13	2.080e-13	2.116e-13	2.176e-13	2.281e-13	2.361e-13	2.199e-13	2.313e-13
50000	1.430e-13	1.430e-13	1.431e-13	1.433e-13	1.437e-13	1.443e-13	1.454e-13	1.473e-13	1.508e-13	1.519e-13	1.352e-13	1.289e-13
100000	8.524e-14	8.524e-14	8.525e-14	8.526e-14	8.529e-14	8.531e-14	8.535e-14	8.541e-14	8.584e-14	8.512e-14	7.384e-14	6.482e-14
	$\alpha_{\text{HeII } 2^2P}^{\text{eff}} [\text{cm}^3 \text{s}^{-1}]$											
3000	2.830e-12	2.844e-12	2.866e-12	2.908e-12	2.995e-12	3.168e-12	3.516e-12	4.244e-12	5.888e-12	1.051e-11	2.671e-11	9.972e-11
5000	1.926e-12	1.931e-12	1.938e-12	1.953e-12	1.985e-12	2.047e-12	2.174e-12	2.433e-12	2.983e-12	4.390e-12	8.497e-12	2.206e-11
7500	1.407e-12	1.409e-12	1.412e-12	1.418e-12	1.432e-12	1.460e-12	1.516e-12	1.631e-12	1.869e-12	2.459e-12	4.036e-12	8.288e-12
10000	1.121e-12	1.123e-12	1.124e-12	1.127e-12	1.135e-12	1.150e-12	1.181e-12	1.246e-12	1.378e-12	1.706e-12	2.551e-12	4.567e-12
12500	9.375e-13	9.383e-13	9.392e-13	9.411e-13	9.457e-13	9.553e-13	9.753e-13	1.016e-12	1.101e-12	1.310e-12	1.846e-12	3.017e-12
15000	8.082e-13	8.088e-13	8.093e-13	8.106e-13	8.136e-13	8.202e-13	8.340e-13	8.624e-13	9.205e-13	1.067e-12	1.442e-12	2.209e-12
20000	6.366e-13	6.369e-13	6.371e-13	6.378e-13	6.394e-13	6.430e-13	6.507e-13	6.666e-13	6.989e-13	7.828e-13	1.001e-12	1.407e-12
30000	4.502e-13	4.503e-13	4.504e-13	4.507e-13	4.514e-13	4.529e-13	4.563e-13	4.633e-13	4.774e-13	5.161e-13	6.232e-13	7.972e-13
50000	2.857e-13	2.858e-13	2.858e-13	2.859e-13	2.862e-13	2.868e-13	2.880e-13	2.907e-13	2.955e-13	3.102e-13	3.570e-13	4.215e-13
100000	1.488e-13	1.488e-13	1.488e-13	1.488e-13	1.489e-13	1.491e-13	1.495e-13	1.503e-13	1.515e-13	1.552e-13	1.720e-13	1.912e-13

Table 4: Command-line arguments for NEBULAR.

Args.	Value	Purpose
-r	min, max, delta [\AA or Hz]	Wavelength / frequency range and step size
-i	input wavelength/frequency table	alternative to -r; ASCII format
-t	electron temperature	
-n	electron density	
-f	H ⁺ , He ⁺ , He ⁺⁺ ion. fractions	optional; calculated internally if omitted
-o	output file name	optional; default: <code>nebular_spectrum.dat</code>
-a	helium abundance ratio by parts	optional; default: 0.10
-c	A or B	optional; Case A/B for emission lines; default: B
-w	FWHM [\AA or Hz]	optional; width of a Gaussian kernel to convolve the spectrum
-b	-	optional; suppresses header lines if given

Table 5: Resulting output of NEBULAR (abridged). The first two columns contain frequencies and wavelengths. The third column is the total spectrum, either f_ν or f_λ . The remaining columns give the free-bound, two-photon, free-free and emission-line components for the various ionic species, respectively.

ν [Hz]	λ [\AA]	f_λ	$j_{\text{fb}}(\text{H I, He I, He II})$	$j_{2q}(\text{H I, He II})$	$j_{\text{ff}}(\text{H I, He I, He II})$	$j_{\text{em}}'(\text{H I, He I, He II})$
6.17238e+14	4857	6.88516e-13	3.39204e-13 ...	1.33683e-13 ...	1.04514e-13 ...	0 ...
6.17111e+14	4858	6.88408e-13	3.39198e-13 ...	1.33591e-13 ...	1.04514e-13 ...	0 ...
6.16984e+14	4859	6.88301e-13	3.39191e-13 ...	1.33500e-13 ...	1.04514e-13 ...	0 ...
6.16857e+14	4860	6.88193e-13	3.39185e-13 ...	1.33409e-13 ...	1.04514e-13 ...	0 ...
6.16730e+14	4861	1.32878e-11	3.39178e-13 ...	1.33318e-13 ...	1.04514e-13 ...	0 ...
6.16603e+14	4862	6.87978e-13	3.39171e-13 ...	1.33226e-13 ...	1.04514e-13 ...	0 ...
6.16476e+14	4863	7.86879e-10	3.39165e-13 ...	1.33135e-13 ...	1.04515e-13 ...	7.8619e-10 ...
6.16350e+14	4864	6.87764e-13	3.39158e-13 ...	1.33044e-13 ...	1.04515e-13 ...	0 ...
6.16223e+14	4865	6.87657e-13	3.39151e-13 ...	1.32953e-13 ...	1.04515e-13 ...	0 ...
6.16096e+14	4866	6.87549e-13	3.39144e-13 ...	1.32863e-13 ...	1.04515e-13 ...	0 ...
6.15970e+14	4867	6.87442e-13	3.39138e-13 ...	1.32772e-13 ...	1.04515e-13 ...	0 ...
6.15843e+14	4868	6.87335e-13	3.39131e-13 ...	1.32681e-13 ...	1.04515e-13 ...	0 ...
6.15717e+14	4869	6.87228e-13	3.39124e-13 ...	1.32590e-13 ...	1.04515e-13 ...	0 ...
6.15590e+14	4870	6.87121e-13	3.39117e-13 ...	1.32500e-13 ...	1.04515e-13 ...	0 ...
6.15464e+14	4871	6.87014e-13	3.39110e-13 ...	1.32409e-13 ...	1.04515e-13 ...	0 ...
6.15338e+14	4872	6.86907e-13	3.39103e-13 ...	1.32319e-13 ...	1.04515e-13 ...	0 ...
6.15211e+14	4873	6.86800e-13	3.39096e-13 ...	1.32229e-13 ...	1.04515e-13 ...	0 ...
6.15085e+14	4874	6.86693e-13	3.39089e-13 ...	1.32139e-13 ...	1.04515e-13 ...	0 ...